Modeling of Crack Formation after Pulse Heat Load in ITER-grade Tungsten

A.S. Arakcheev[1,2,3,a)], A.V. Burdakov[1,3], A. Huber[4], A.A. Kasatov[1], A. Kreter[4], Ch. Linsmeier[4], Th. Löwenhoff[4], Ph. Mertens[4], A.A. Shoshin[1,2], D.I. Skovorodin[1,2], A.A. Vasilyev[1,2], L.N. Vyacheslavov[1,2] and M. Wirtz[4]

[1]*Budker Institute of Nuclear Physics SB RAS, 11 akademika Lavrentieva , Novosibirsk 630090, Russia.*
[2]*Novosibirsk State University, 2 Pirogova str., Novosibirsk 630090, Russia.*
[3]*Novosibirsk State Technical University, 20 K. Marksa prospect, Novosibirsk 630090, Russia.*
[4]*Forschungszentrum Jülich GmbH, Institut für Energie- und Klimaforschung - Plasmaphysik, 52425 Jülich, Germany.*

[a)]Corresponding author: asarakcheev@gmail.com

Abstract. The one-dimensional numerical simulations of the deformation during and after the pulsed heat load are carried out for tungsten manufactured according to ITER specifications. The calculations for stress-relieved tungsten demonstrated the cracking at temperatures above ductile-to-brittle transition temperature. The features of the stresses caused by thermal expansion are discussed.

INTRODUCTION

Currently, the first wall and divertor in ITER are believed to suffer from continuous and pulsed thermal loads [1]. Experimental studies demonstrated mechanical destruction of materials to occur at power densities above a certain threshold [2]. The crack formation in tungsten is observed after pulsed heat loads [3, 4]. The tungsten at temperature above ductile-to-brittle transition temperature is supposed to be resistant to cracking [5, 6]. However, the properties of tungsten manufactured according to ITER specifications are specific. The paper is aimed at calculation of the cracking conditions for the tungsten and discussion of the features of the failure after pulsed heat loads [7].

MATHEMATICAL MODEL

In this section we will discuss the mathematical models of the simulated physical processes and used assumptions and approximations.

All numerical simulations are carried out at the one-dimensional approach. The approach usually is valid due to the small crack depth and distance of temperature propagation during the heating relatively to the typical size of irradiated area. Thus, all material parameters are supposed to depend only on the distance to the surface. However, the approach become invalid after the crack formation. So, the model may be used for the calculation of the conditions of the crack formation but not for the accurate calculation of the crack parameters.

Temperature propagation

We will assume the distance to be much smaller than the thickness of the material. Then the temperature distribution is described by the heat equation

$$C_p(T)\rho\frac{\partial T(z,t)}{\partial t} = \frac{\partial}{\partial z}\left(\lambda(T)\frac{\partial T(z,t)}{\partial z}\right), \tag{1}$$

the boundary condition

$$\lambda(T)\frac{\partial T(0,t)}{\partial z} = -W(t) \tag{2}$$

and the initial condition

$$T(z, 0) = T_0, \tag{3}$$

where T is the temperature; z is the surface normal coordinate; t is the time; C_p is the specific heat capacity; ρ is the density; λ is the thermal conductivity; W is the heating power density; T_0 is the initial (base) temperature.

The heat equation was solved numerically with the thermodynamic parameters of the tungsten manufactured according to ITER specifications [7] for a temperature increase up to 2000°C, a heating duration of 0.1ms to 5ms, an initial temperature of 0°C to 2000°C, and a maximum temperature of up to 3000°C. In the area of interest, the discrepancy between the computational maximum temperature and the analytical expression does not exceed 70°C:

$$T_{max}[^\circ\mathrm{C}] \approx T_0[^\circ\mathrm{C}] + 2\sqrt{\tau[\mathrm{ms}]}W[\mathrm{MW/m^2}]. \tag{4}$$

Hereinafter we will use this approximated formula.

Elastic deformation under pulsed heat load

The problem of finding the elastic deformation and stresses when the temperature distribution is non-uniform includes the mechanical equilibrium equation

$$\frac{\partial \sigma_{ij}}{\partial x_j} = 0, \tag{5}$$

force-free boundary condition

$$\sigma_{ij} n_j = 0 \tag{6}$$

and Hooke's law

$$\sigma_{ij} - E(T)\left(\frac{1}{1+\nu(T)}\varepsilon_{ij} + \frac{\nu(T)}{(1+\nu(T))(1-2\nu(T))}\varepsilon_{ll}\delta_{ij}\right) = -\frac{E(T)}{1-2\nu(T)}u(T, T_0)\delta_{ij}, \tag{7}$$

where σ_{ij} is the stress tensor; n_j is the normal to the surface; E is Young's modulus; ν is the Poisson coefficient; ε_{ij} is the deformation tensor; $u(T, T_0)$ is the elongation at the temperature T relative to the size at the temperature T_0 [8]. With constant linear coefficient of thermal expansion α

$$u(T, T_0) = \alpha(T - T_0). \tag{8}$$

The linear elasticity problem has an exact analytical solution [5]:

$$\sigma_{zz} = \sigma_{xy} = \sigma_{xz} = \sigma_{yz} = 0, \tag{9}$$

$$\sigma_{xx} = \sigma_{yy} = -\frac{E(T(z))}{1-\nu(T(z))}u(T(z), T_0). \tag{10}$$

The arising displacements are directed only perpendicular to the surface of the material. This solution has the important feature of taking the temperature dependence of mechanical properties into account. Note that the mode of deformation is principally different from the case of the formation of similar stresses by the application of a mechanical force. The latter always is accompanied by an expansion along the surface. The difference corresponds to the inequality of the tensile test and the effect of the pulsed heat load. Another difference is the simultaneous change of the deformation and the material properties caused by the change of the temperature.

In the presence of plastic deformation, expressions (9) and (10) will be wrong. However, due to the homogeneity of the problem along the material surface, the plastic deformation of the surface layer will not lead to appearance of displacements along the surface.

Model of plastic deformation

We will describe the plastic deformation using the Hollomon equation [9, 10]:

$$\sigma = K\varepsilon_p^n, \tag{11}$$

where σ is the stress; K is the strength coefficient; ε_p is the plastic relative deformation; n is the strain-hardening exponent. Initially this equation was used for description of elongation in uniform one-axis extension. We will apply it to both compression and extension, using the same values of strength coefficient and strain-hardening exponent, because experimental data are available only for plastic extension [7].

In addition, we will use the fact that plastic deformation occurs with no change in the specific volume of the material and that hydrostatic compression does not cause plastic deformation [11]. It defines the relations of the components of the plastic part of the deformation tensor:

$$\varepsilon^p_{xx} = \varepsilon^p_{yy} = -\frac{1}{2}\varepsilon^p_{zz}. \tag{12}$$

TEMPORAL BEHAVIOR OF DEFORMATION AND STRESS

To calculate the temporal dependence of the stresses we use the absence of a displacement along the material surface caused by the one-dimensional approach:

$$\varepsilon_{xx} = 0. \tag{13}$$

This extension consists of three parts (thermal expansion, elastic and plastic deformation):

$$u(T, T_0) + \varepsilon^e_{xx} + \varepsilon^p_{xx} = 0. \tag{14}$$

The elastic and plastic deformations may be expressed as functions on the mechanical stress using the discussed models. Thus the formula (14) connects temporal behavior of the temperature and stresses.

CRACKING CONDITION

Assuming the heating from the initial temperature T_0 to maximal temperature T_{max} and cooling down back the residual tensile stress may be calculated as a function of T_0 and T_{max}. It is convenient to substitute the maximum temperature using the expression (4). The numerical calculations are based on the data for tungsten manufactured according to ITER specifications that are given in [7]. The calculation results are available only for a maximum temperature of up to 2500°C, as there is no data on the mechanical properties of tungsten for higher temperatures.

Cracks arise if the stress in the material after a heating-cooling cycle exceeds the ultimate tensile strength (UTS). Note that the stress should be compared with the ultimate tensile strength at the base temperature. Figure 1 presents results of such comparison.

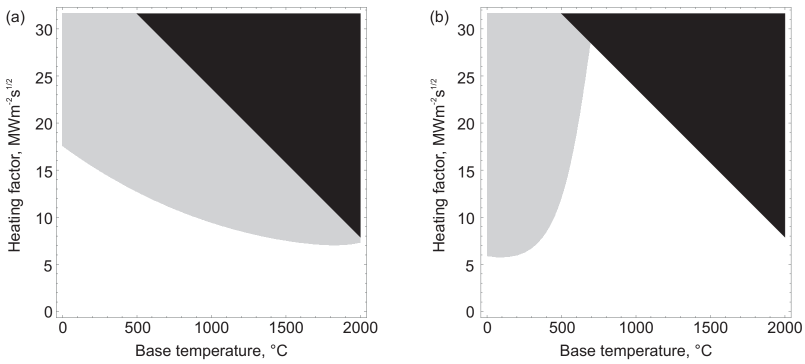

FIGURE 1. Results of heating tungsten manufactured according to ITER specifications after heating-cooling cycle as numerically calculated vs. initial temperature T_0 and heating factor F_{HF}. Grey region: crack formation; black region: no data on mechanical properties. (a) Stress-relieved tungsten, (b) Annealed tungsten.

DISCUSSION

Numerical simulations of deformations during pulsed heat loads were carried out for tungsten manufactured according to the ITER specifications using the data from [7]. The conditions of the crack formation in terms of the base temperature and heating factor ($F_{HF} = W\sqrt{\tau}$) were obtained (Figure 1). Due to a higher UTS, the calculated energy threshold of cracking for the stress-relieved tungsten is about three times higher than the one for annealed material. However, increasing of the base temperature leads to decrease in the threshold for stress-relieved material. The behavior contradicts to a usual feature of the tungsten and tungsten alloys: the growth of the threshold with increase in the base temperature (Figure 1(b)). The feature of the stress-relieved ITER-grade tungsten causing the low resistivity to pulsed heat loads at high base temperatures is the high yield strength. Formally, the ductile-to-brittle transition temperature of the stress-relieved tungsten is about 400°C. It means that at this temperature the UTS equals a 0.2% yield strength. However, at any temperature the yield strength is close to the UTS [7]. The ductile-to-brittle transition is a gradual process - the deformation at which the material fractures gradually grows with the temperature. To ensure resistance to crack formation the yield strength should be much less than the UTS.

Another result of the calculations of stresses and deformations is the found qualitative difference of the deformation during the pulsed heat loads and tensile test. The thermal expansion leads to a displacement perpendicular to the surface. Application of a tensile force causes expansion along the direction of the force (along the material surface). The difference is not significant for a uniform material. However, the results of the tensile tests may demonstrate a better failure strength of fiber-reinforced materials, while the energy threshold of cracking under pulsed heat loads is not improved. The different behaviors are caused by the different deformations. In the case of tensile test the higher stiffness of fibers oriented along the direction of the force applied could improve the material strength because stiffer fibers extend with the material. Otherwise, in the case of pulsed heat load the stresses are oriented along the surface, while the displacement is perpendicular to it. So, fibers along the surface cannot help to reduce stress in material. Fibers perpendicular to the surface can also change the situation only if their thermal expansion coefficient significantly differs from the material one. All in all, the fiber-reinforcement cannot improve the threshold of crack formation after a pulsed heat load. Still, the fibers may slow down the propagation of cracking.

SUMMARY

The one-dimensional numerical simulations of the deformation during and after the pulsed heat load are carried out for tungsten manufactured according to ITER specifications. The plasticity is taken into account using the Hollomon equation and approach of kinematic hardening. The calculations for stress-relieved tungsten demonstrated the cracking at temperatures above ductile-to-brittle transition temperature. The effect is caused by closeness of UTS and yield strength of the tungsten. To prevent the crack formation the material of the fusion reactor divertor plates should be ductile. It means the yield strength should be much less than ultimate tensile strength.

The pulsed heat load leads to almost only perpendicular to surface displacement. It means the fibers along the surface are not stretched during the loads. So, fiber-reinforcement does not improve the energy threshold of the crack formation under the pulsed heat loads.

Currently, the discussed model of cracking can be used for calculation of cracking conditions after one heating-cooling cycle. The tacking into account of the material fatigue for the multi-cycle loads calculation is prospected. The numerical simulation of the parallel to surface cracks requires using of two-dimensional model and accurate calculation of stresses near the crack.

ACKNOWLEDGEMENTS

This work was supported by Russian Science Foundation (project N 14-50-00080).

REFERENCES

[1] G. Janeschitz, K. Borrass, G. Federici, Y. Igitkhanov, A. Kukushkin, H.D. Pacher, G.W. Pacher, M. Sugihara, J. Nucl. Mater. **220-222**, 73-88 (1995).

[2] V.T. Astrelin, A.V. Burdakov, P.Z. Chebotaev, V.V. Filippov, V.S. Koidan, K.I. Mekler, P.I. Melnikov, V.V. Postupaev, A.F. Rovenskikh, M.A. Shcheglov, H. Wuerz. Nucl. Fusion, 37(11), 1541-1558 (1997).

[3] A.A. Vasilyev, A.S. Arakcheev, I.A. Bataev, V.A. Bataev, A.V. Burdakov, I.V. Kandaurov, A.A. Kasatov, V.V. Kurkuchekov, K.I. Mekler, V.A. Popov, A.A. Shoshin, D.I. Skovorodin, Yu.A. Trunev, L.N. Vyacheslavov, "Observation of the Tungsten Surface Damage under ITER-relevant Transient Heat Loads during and after Electron Beam Pulse", AIP Conf. Proc. (these proceedings).

A.V. Arzhannikov, V.A. Bataev, I.A. Bataev, A.V. Burdakov, I.A. Ivanov, M.V. Ivantsivsky, K.N. Kuklin, K.I. Mekler, A.F. Rovenskikh, S.V. Polosatkin, V.V. Postupaev, S.L. Sinitsky, A.A. Shoshin. J. Nucl. Mater., 438, S677-S680 (2013).

[4] A. Huber, A. Arakcheev, G. Sergienko, I. Steudel, M. Wirtz, A.V. Burdakov, J.W. Coenen, A. Kreter, J. Linke, Ph. Mertens, V. Philipps, G. Pintsuk, M. Reinhart, U. Samm, A. Shoshin, B. Schweer, B. Unterberg, M. Zlobinski, Phys. Scr., T159, 014005 (2014).

[5] A.S. Arakcheev, A. Huber, M. Wirtz, G. Sergienko, I. Steudel, A.V. Burdakov, J.W. Coenen, A. Kreter, J. Linke, Ph. Mertens, A.A. Shoshin, B. Unterberg, A.A. Vasilyev, J. Nucl. Mater. **463**, 246-249 (2015).

[6] A.S. Arakcheev, D.I. Skovorodin, A.V. Burdakov, A.A. Shoshin, S.V. Polosatkin, A.A. Vasilyev, V.V. Postupaev, L.N. Vyacheslavov, A.A. Kasatov, A. Huber, Ph Mertens, M. Wirtz, Ch Linsmeier, A. Kreter, Th Lowenhoff, L. Begrambekov, A. Grunin, Ya Sadovskiy, J. Nucl. Mater. **467**, 165-171 (2015).

[7] ITER Materials Properties Handbook (MPH), Part 1 (internal project document distributed to the ITER Participants).

[8] L.D. Landau, E.M. Lifshitz, Theory of Elasticity (Pergamon Press, 1970).

[9] J.H. Hollomon, Transactions of the American Institute of Mining, Metallurgical and Petroleum Engineers **162**, 268-290 (1945).

[10] Z. Zhongping, W. Weihua, C. Donglin, S. Qiang, Z. Wenzhen, J. Mater. Eng. Perform **13**(4), 509-512 (2004).

[11] L.M. Kachanov, Foundations of the theory of plasticity (North-Holland Publishing Company, Amsterdam 1971).

[12] "Report on the Mechanical and Thermal Properties of Tungsten and TZM Sheet Produced in the Refractory Metal Sheet Rolling Program", Part 1, Southern Research Institute, SR-66H31 (AD-638631), 1966.